

# RESPONSE OF A COSMIC RAY DETECTOR TO Cf-252 FISSION FRAGMENTS AND THE DESIGN OF A ROTATING SCATTERING CHAMBER

Jason Alicea\*

Department of Physics, University of Florida

A cosmic ray particle identifier consisting of a thin film detector (for measuring specific luminescence) and a solid state detector (for measuring residual energy) has been designed to simultaneously measure the nuclear charge, mass, velocity, energy, and possibly ionic charge of incident particles. A 10-layer thin film was fabricated and tested in this identifier. The response of both the thin film and the solid-state detectors to Cf-252 fission fragments was measured. As expected, the thin film detector yielded a very wide peak in its specific luminescence spectrum, resulting in an uncertainty in Z detection of  $\pm 2$ . In contrast, the solid-state detector signal had a much narrower peak and is thus capable of adequately precise energy measurement. Also presented is the design of a rotating scattering chamber used to scatter the particle beam from the Van de Graaff accelerator through a thin foil at an angle between  $0^\circ$  and  $60^\circ$ . The scattering chamber will reduce the intensity of the beam, which at present is too high for the solid-state detector and electronics. Machine drawings have been submitted for its construction, although its fabrication is not yet underway.

## 1. INTRODUCTION

In the early part of the 20<sup>th</sup> century, the German physicist Victor F. Hess discovered that corpuscular radiation (e.g., alpha and beta particles) continuously bombards the earth from outer space [1]. The properties of these “cosmic rays” vary enormously. For instance, cosmic ray energies range from  $10^9$ eV to  $10^{19}$ eV. Cosmic rays also vary enormously in intensity, with low-energy radiation occurring much more frequently than high-energy radiation [1]. The radiation includes elements ranging from hydrogen to much heavier elements (i.e.,  $Z \geq 10$ ), and moreover, these elements range from possessing little or no ionic charge to being stripped down to bare nuclei. In addition, the frequency of these elements varies greatly, with hydrogen nuclei comprising the vast majority of cosmic rays (see Table I)

---

\* Supported by the NSF and University of Florida REU Program.

[2]. Naturally, it would be desirable to have a cosmic ray detector that is capable of measuring simultaneously the ionic and nuclear charge, mass, velocity, and energy of incident radiation. Such a detector could provide insight into the nature, composition, and origin of cosmic rays.

*Table I.* Number of various nuclei per 100,000 hydrogen nuclei in the cosmic radiation.

<b>Nuclei</b>	<b>Z</b>	<b>Relative Number</b>
Hydrogen	1	100,000
Helium	2	6,770
Light nuclei	3 to 5	146
Medium nuclei	6 to 9	430
Heavy nuclei	$\geq 10$	246

Dr. M. L. Muga of the University of Florida Chemistry Department has designed a low-mass detector of modest power requirements and reasonable cost to simultaneously measure these properties of the corpuscular radiation, particularly the heavy-mass, low-energy portion. This particle identifier can roughly be divided into two sections: a thin-film detector (TFD) and a solid-state detector (SSD), and is thus referred to as a TFD-SSD system.

Laboratory experiments testing the detector involve either a Van de Graaff accelerator or Cf-252 fission fragment source for test particles. A particle entering the TFD-SSD from either source first passes through the TFD, which contains a thin, self-supporting scintillator film mounted on a celluloid frame that luminesces (emits photons) when a particle traverses the film. Adjacent photomultiplier (PM) tubes then absorb these photons and convert this light signal into an electronic signal and amplify it, allowing acquisition of luminescence data. The particle then enters the SSD, where it stops. The SSD detector measures the residual energy of the particle.

From this data, the properties of the particle can be extrapolated as follows. A model of the specific luminescence<sup>1</sup> ( $\Delta L/\Delta x$ ) vs. energy reveals a curve that is specific to the atomic number Z of each particle. When particles of a given mass and energy pass through the

---

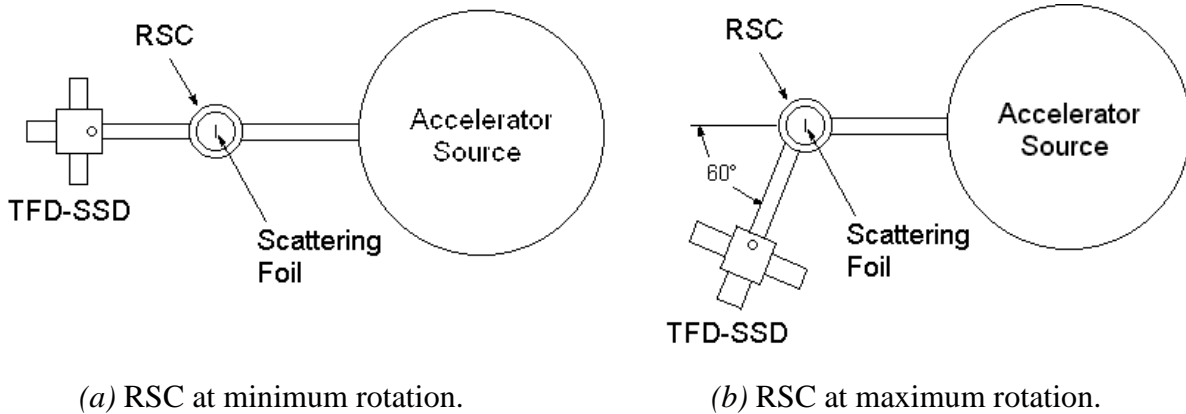
<sup>1</sup> Specific luminescence is simply the luminescence L per unit thickness of the thin scintillator film.

detector, the recorded luminescence and energy yield a point on this graph. The curve that the point lies on gives the atomic number  $Z$  of these particles. The velocity of the particle can be calculated by taking the distance between the thin scintillator film and the SSD and dividing by the time recorded between signals from the TFD and SSD. The mass can subsequently be easily determined using the measured energy and velocity of the particle. Ionic charge detection is still speculative, although the experimenters believe that using a detector with multiple TFDs, ionic charge can be determined by comparing the specific luminescence and velocity measured after each thin film.

Eventually, the investigators hope to use this detector on a space mission and obtain data on heavy-mass, low-energy cosmic rays, as the detector's dependability, moderate cost and power requirements, low mass, and diverse measuring capability render it an excellent candidate for space instrumentation.

My involvement in the experiment this summer was twofold. First, I fabricated a 10-layer thin film for the TFD and with it obtained data from the detector using alpha particles that decayed from a radioactive Cf-252 source. The second project I participated in along with Brad Smrstick, a high school physics teacher participating in the Teacher Research Update Experience (TRUE) program, was the design of a rotating scattering chamber (RSC). The motivation for this project is that the SSD and electronics cannot safely withstand a high-intensity beam (on the order of nanoamps). Although the beam can be attenuated to safe levels directly from the accelerator by defocusing the beam or cutting back on the gas pressure in the accelerator terminals, adjusting it in this fashion results in a loss of control over the beam. The RSC will scatter the beam off one of the foils in the chamber through an angle between  $0^\circ$  and  $60^\circ$  degrees, thereby adequately reducing the beam intensity due to Rutherford scattering without loss of control of the beam. Figs. 1a and 1b show schematic representations of the accelerator, RSC, and TFD-SSD at the minimum and maximum rotation angles, respectively.

Figure 1.



## 2. TFD-SSD EXPERIMENT

### 2.1 Experimental Setup

Figs. 2 and 3 show a photograph and schematic drawing, respectively, of the TFD-SSD. The TFD consists of two PM tubes and a thin, self-supporting scintillator film made of two layers of VYNS<sup>2</sup> for stability and between 4 and 16 layers of NE-102<sup>3</sup> scintillator. The film, whose mass per unit area<sup>4</sup> is approximately  $100\mu\text{g}/\text{cm}^2$ , is mounted on a square celluloid frame. The thin film is housed in a horizontal cylindrical cavity inside a cubic aluminum chamber. Adjacent to the film on opposing sides are the two PM tubes. The SSD is located at the end of the detector in a cylindrical chamber. The planes of both the thin film and SSD are oriented perpendicular to the path traversed by impinging particles.

<sup>2</sup> Solution is obtainable from Nuclear Enterprises, Inc., San Carlos, CA.

<sup>3</sup> Solution is obtainable from Pilot Chemicals Div., New England Nuclear Corp., Watertown, Mass.

<sup>4</sup> Nuclear physicists often use mass per unit area to describe the thickness of a material when both the geometric thickness and density are important quantities.



Figure 2. Photograph of the TFD-SSD.

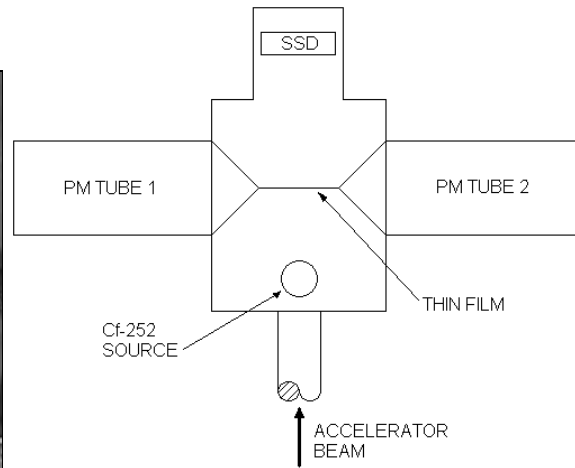


Figure 3. Schematic of the TFD-SSD.

In experiments conducted this summer, a Cf-252 fission fragment source was used to test the TFD-SSD. The Cf-252 source is connected to a vertical plunger located in front of the TFD. When the plunger is raised, no radiation passes through the TFD or SSD. The plunger is lowered only when running the experiment or testing the detector.

The detector must be kept at vacuum pressure in order to eliminate interactions between incoming particles and air molecules. A mechanical pump evacuates the chamber to roughly  $10^{-3}$  torr.

Signals are obtained from both PM tubes and the SSD and sent through a series of electronics in order to amplify and shape the signals and reduce noise. Fig. 4 shows a schematic representation of the electronics setup. Although initially there are three individual signals (one from each PM tube and one from the SSD), the signals from the PM tubes are mixed in the dual linear delay amplifier, thereby reducing the number of signals to two. After these two signals are passed through biased amplifiers, they are sent individually to the data analysis computer (DAC) for data acquisition.

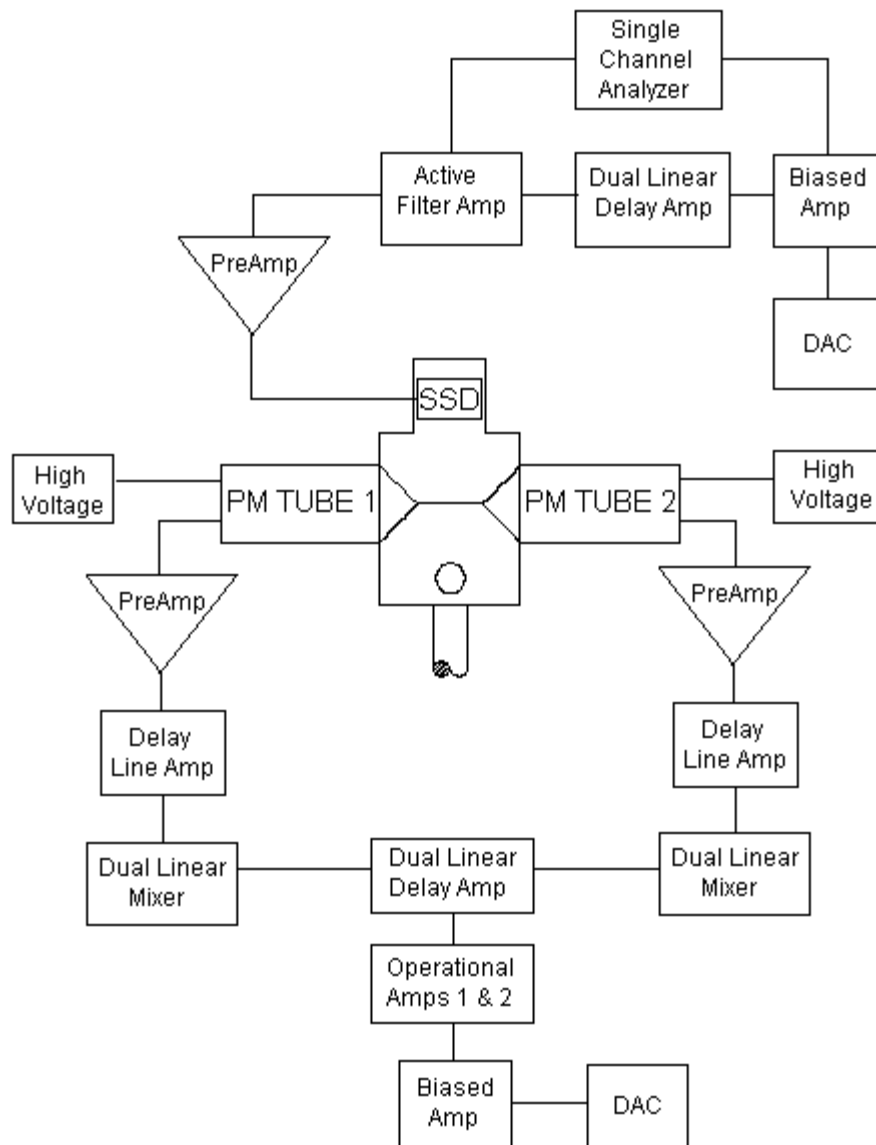


Figure 4. Schematic of the electronics setup.

## 2.2 Detector Theory

A particle from either an accelerator source or fission fragment source first passes through the thin scintillator film in the TFD-SSD. Due to Coulombic interactions, transiting particles excite  $\pi$  electrons in the NE-102 scintillator. When these electrons decay back to their previous energy levels, they emit light—mostly visible but close to ultraviolet—

uniformly over a  $4\pi$  solid angle. The cylindrical chamber reflects many of these photons until they are absorbed by the PM tubes.

The PM tubes then convert the light to an electronic signal and amplify it as follows. The inside glass face on the end of each PM tube is coated with CsI. When photons from the NE-102 pass through this coating, they free electrons in the CsI by the photoelectric effect. The inner portion of the PM tubes contains a series of electrodes, each at successively higher potential, with the electrode closest to the lens at the lowest potential (see Fig. 5). Therefore, free electrons from the CsI accelerate toward the first electrode, where they free more electrons. These electrons then accelerate toward the next electrode, which is at an even higher potential, and thus free more electrons. This process repeats until the electrons reach the end of the PM tube. The accumulated charge is then sent into the preamplifier and subsequent electronics (refer to Fig. 4) for signal processing. The DAC then obtains the specific luminescence from the scintillator induced by the transiting particle.

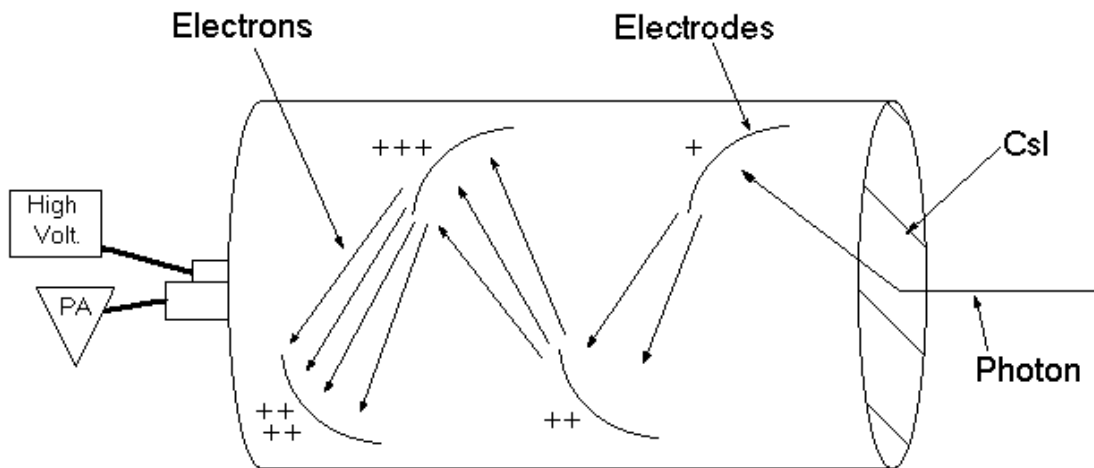


*Figure 5.* Schematic of a PM tube.

The computer records a number of events, typically on the order of  $10^5$ , and builds a curve of counts vs. specific luminescence (Fig. 6) for a particle of given Z. One can obtain the

average specific luminescence of these particles by taking the specific luminescence value that corresponds to the peak of the curve.

After passing through the TFD, the particle enters the SSD, which consists of a silicon semiconductor coated with a thin gold layer for electrical contact. Here the particle ionizes in the silicon, with the amount of ionization proportional to the residual energy of the particle. At the end of the SSD, the charge is collected and the signal sent to the preamplifier and subsequent electronics for amplification and shaping and the DAC for data acquisition. For each particle for which specific luminescence data are taken, residual energy data from the SSD are also taken. The DAC builds a curve similar to that obtained from the TFD of counts vs. residual energy (Fig. 7). Again by taking the energy value corresponding to the peak of this curve, one can obtain the average energy of these particles.

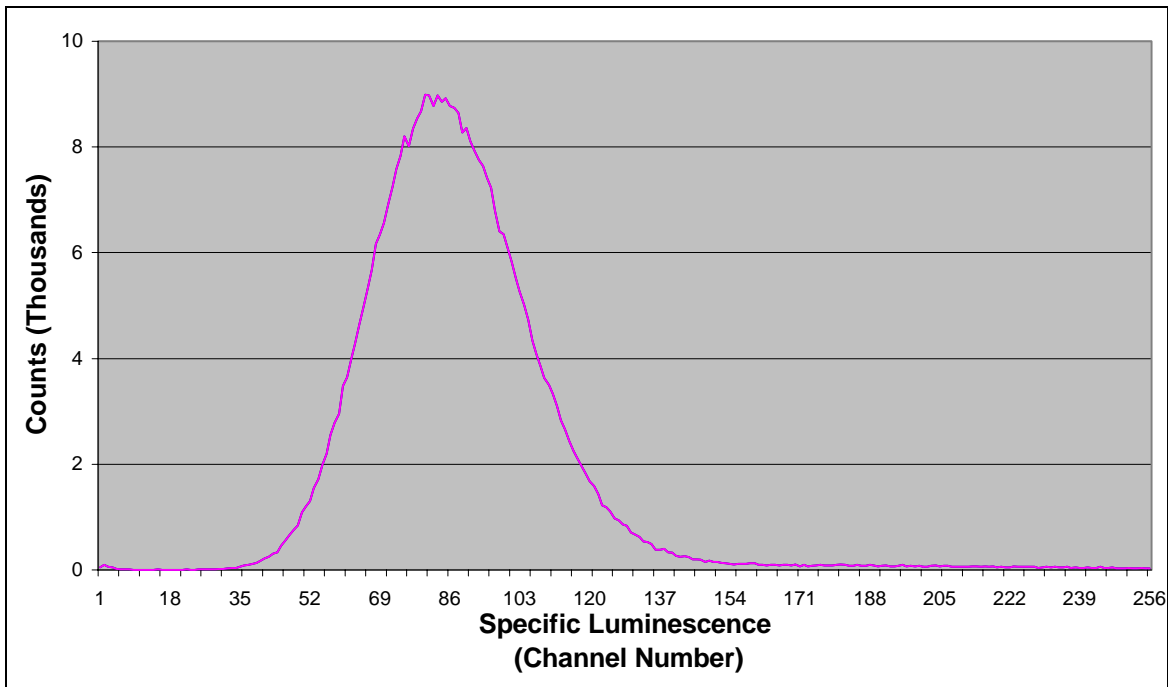
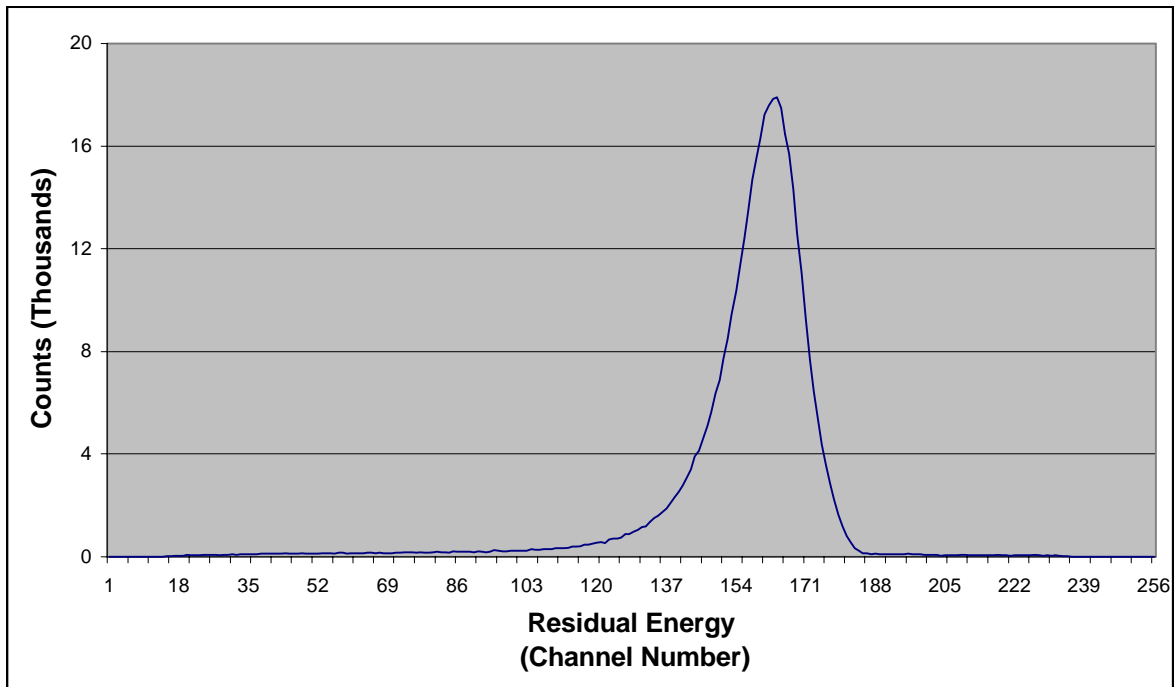


Figure 6. TFD signal recorded by the DAC using a 10-layer thin film and Cf-252 fission fragment source for test particles.



*Figure 7.* SSD signal recorded by the DAC using a Cf-252 fission fragment source for test particles.

In order to extrapolate  $Z$  from the measured data, models must first be constructed for the specific luminescence vs. energy for particles of different  $Z$ , utilizing the fact that these curves are unique for each  $Z$ . Such curves can be obtained by theoretical modeling, from empirical data, or both. Curves can be obtained from empirical data by testing particles of known  $Z$  with several different known energies in the TFD-SSD, plotting the recorded specific luminescence-residual energy points for each energy tested, and fitting a curve through these points. Fig. 8 shows an example of theoretical models and empirical data points for Kr-84 and Ar-40 atoms and illustrates the agreement between them [3]. Both methods may be utilized by recording several experimental data points and then calibrating the theoretical curve to fit them.

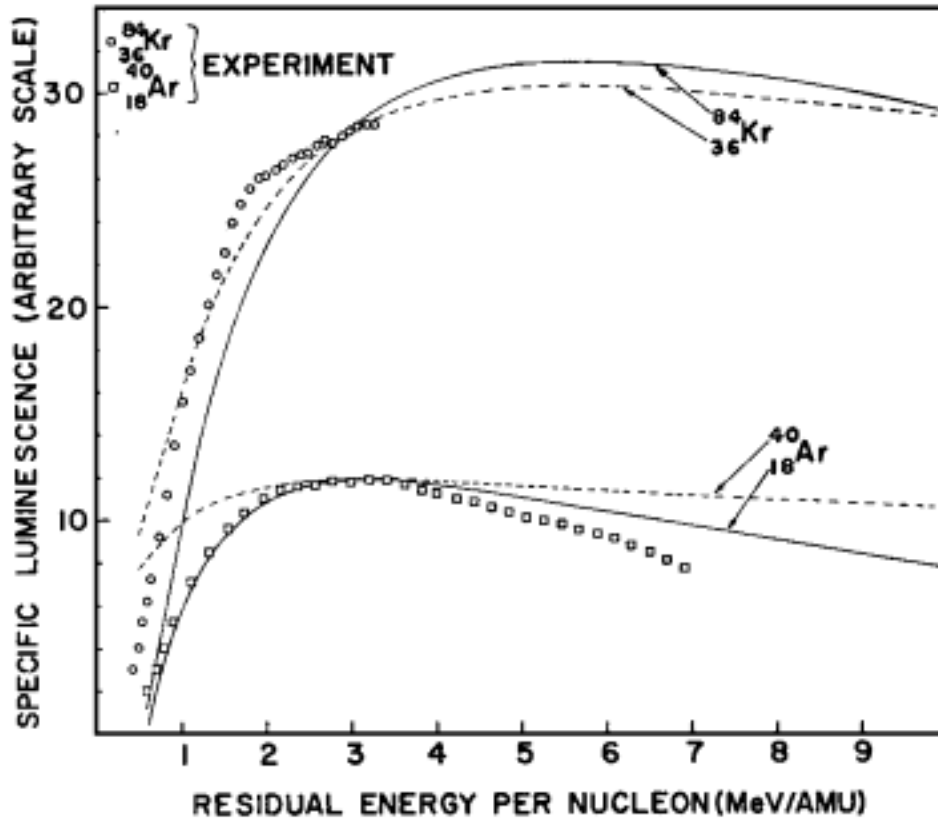


Figure 8.  $\Delta L/\Delta x$  vs. residual energy. Solid and dashed curves are theoretical models; squares (Ar) and circles (Kr) represent empirical data points.

Once the models are obtained, the specific luminescence-residual energy point measured by the TFD-SSD can be plotted on a graph containing these curves. Since each curve corresponds to a different  $Z$ , the curve that this point lies on gives the atomic number of the particle in question.

Another electronics board, a time-to-digital converter (not used in the current experimental setup) measures the time between signals from the TFD and SSD. Since particles do not experience any acceleration in their travel from the thin film to the SSD, one can calculate their velocity by dividing the distance between the thin film and SSD by the measured time between signals. Once the velocity  $V$  and energy  $E$  of the particles are known, one can easily calculate their mass,  $M=2E/V^2$ .

Ionic charge detection is thought to be possible using multiple TFDs and time-to-digital converters to measure the velocity of a particle after it has traversed each thin film. The experimenters believe that a neutral particle will produce the same luminescence signal when passing through each thin film and have a constant velocity after each. Conversely, a highly charged particle will pick up electrons in each thin film and therefore produce weaker luminescence signals in each TFD and have a decreasing velocity after each film. Using this hypothesis, the TFD-SSD is expected to be capable of ionic charge detection.

### **2.3 Experiment**

For the TFD-SSD test conducted this summer, I fabricated a two-layer VYNS, eight-layer NE-102 thin film that was inserted into the TFD. Using the aforementioned experimental setup, fission fragments from the Cf-252 source (the energy of which is known to be roughly 6.1MeV) were used to test the resolution of the TFD with this 10-layer thin film. The DAC recorded specific luminescence and residual energy data of roughly 415,000 particles and built the curves shown in Figs. 6 and 7. No further data analysis took place.

Comparison of Figs. 6 and 7 reveals that the peak in the counts vs. specific luminescence graph is much wider than that in the counts vs. residual energy graph. This result is typical, for the TFD yields a weak signal relative to the SSD due to the small percentage of light captured by the PM tubes and weak luminescence from the thin film. This is a major source of error in these experiments, resulting in an uncertainty of  $\pm 2$  in Z determination for particles tested in the laboratory. (The detector is believed to measure Z for heavy-mass, low-energy cosmic rays more accurately, because at higher Z and lower E there is a greater spacing between the specific luminescence vs. energy curves.) The TFD signal may be strengthened by increasing the number of NE-102 layers, thereby allowing more luminescence. However, this results in a greater energy loss of the particle traversing the thin film, thereby creating experimental error in energy measurements. The TFD signal may also be strengthened by using three sequential TFDs, which previous experiments have shown to reduce the width of the peak at half the maximum value by 54% while not resulting in a significant uncertainty in energy measurement [4].

### 3. ROTATING SCATTERING CHAMBER

As previously mentioned, accelerator sources such as the Van de Graaff can damage the SSD and overload the electronics if their beam intensity is too high. Attenuating the intensity directly results in loss of control of the beam. In order to circumvent this problem, Dr. Muga outlined a design of the RSC introduced earlier. Before this project proceeded, however, I performed a Rutherford scattering calculation to verify that scattering the beam off a foil would adequately reduce the intensity.

The calculation was performed assuming alpha particles scattered off a gold foil of thickness  $\Delta s = 5.2 \times 10^{-8}$  m (mass per unit area =  $100 \mu\text{g}/\text{cm}^2$ ). The energy  $E$  of the alpha particles was assumed to be 4 MeV and the distance  $r$  between the foil and the thin film to be 20 cm. With this configuration, we sought the ratio  $\eta(\phi)/\eta_o$ , the fraction of alpha particles scattered on a unit area at an angle  $\phi$ . According to Rutherford's scattering equation,

$$\eta(\phi)/\eta_o = 1/\sin^4(\phi/2) [N\Delta s (Z_{\text{Au}}Z_{\alpha}e^2/E4\pi\epsilon_o)^2/16r^2],$$

where  $N$  is the number of nuclei per unit volume of gold [5]. Inserting the appropriate data, we found  $\eta(10^\circ)/\eta_o = 2.8 \times 10^{-5}$ ,  $\eta(15^\circ)/\eta_o = 5.5 \times 10^{-6}$ , and  $\eta(20^\circ)/\eta_o = 1.8 \times 10^{-6}$  particles/ $\text{cm}^{-2}$  and concluded that the beam would indeed be sufficiently attenuated in the RSC (the SSD and electronics can safely withstand 1000 counts/sec).

Once these calculations verified the usefulness of the RSC, Brad Smrstick and I finalized the design and drew up the machine drawings necessary to create it. In its final design, the RSC consists of a stationary cylinder and incoming beam pipe around which a collar and outgoing beam pipe rotate. In the radial center of the fixed cylinder are five thin foils connected to a plunger that serves to adjust the height of these targets. The RSC will attach to the Van de Graaff accelerator (or another accelerator source from which experimental data are obtained) on the fixed end and the TFD-SSD on the rotating end. Fig. 9 shows a sketch of the RSC assembly. Fig. 10 shows the design of the fixed cylinder with the

beam pipe from the accelerator. Figs. 11-13 (drawn by Brad Smrstick) show the design of the rotating collar with the beam pipe to the TFD-SSD.

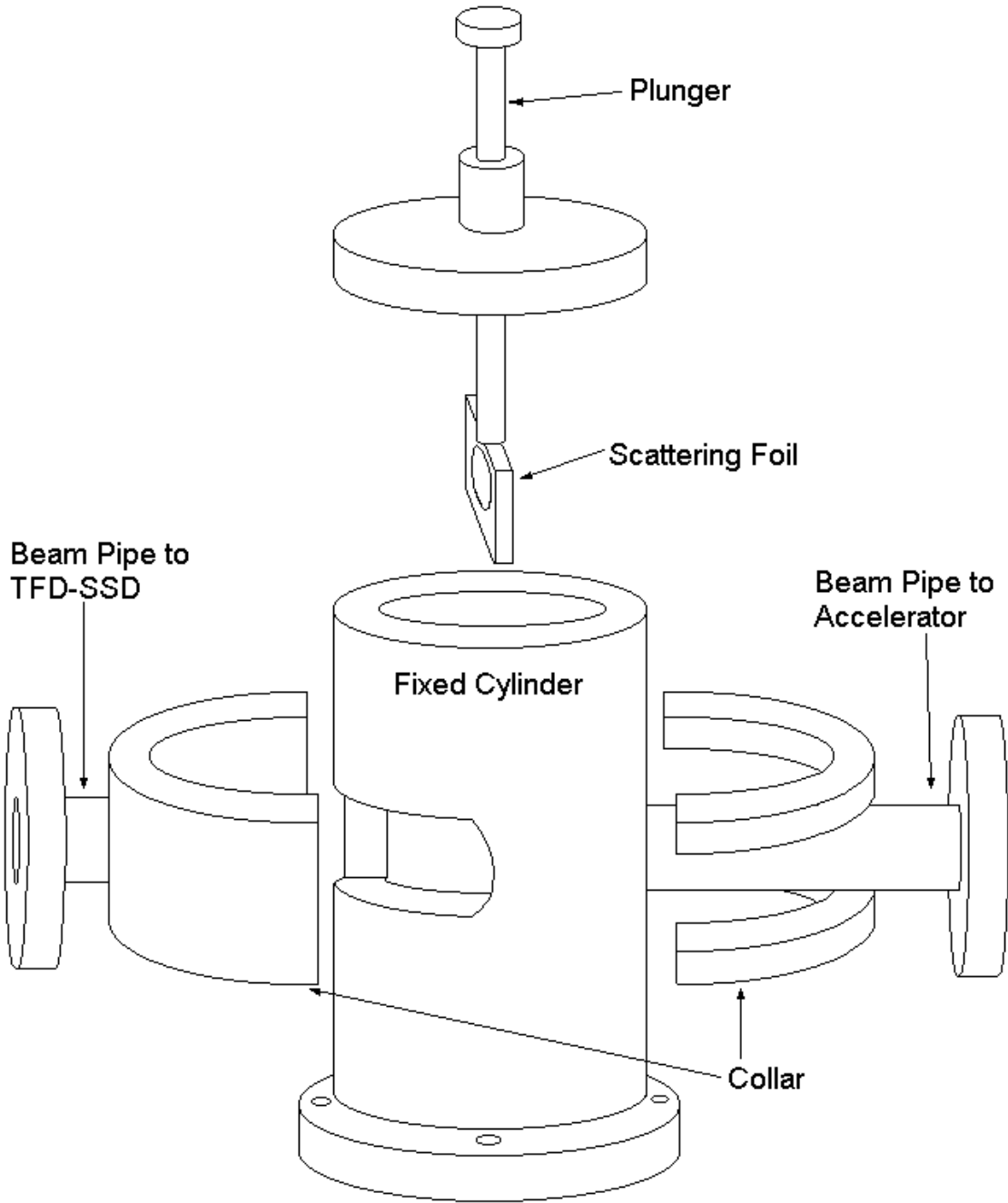


Figure 9. Schematic of the RSC assembly.



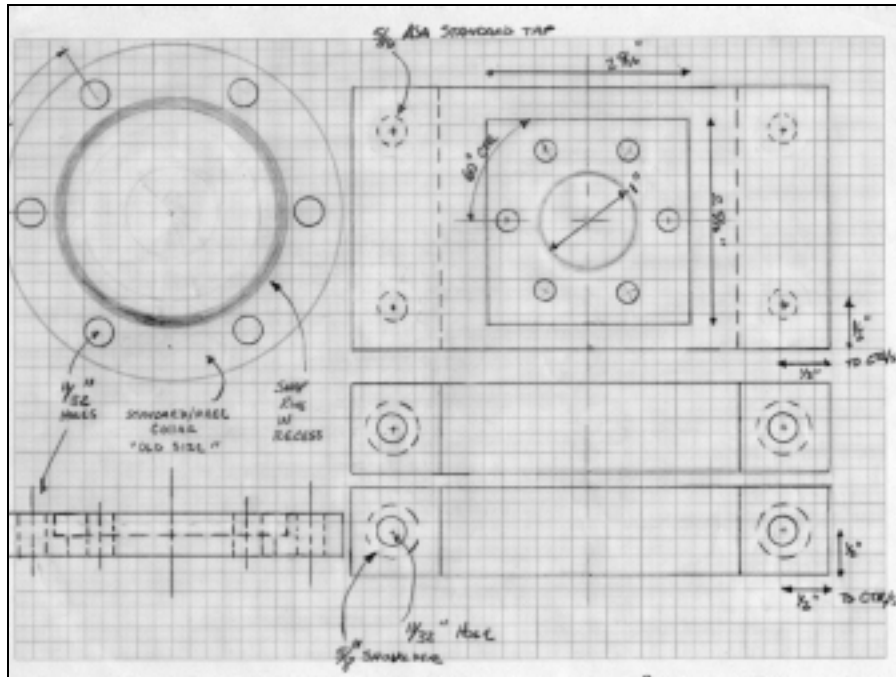


Figure 13. Front view of the collar.

Several requirements needed to be satisfied by this design. First, the RSC must be maintained at vacuum pressure since both the accelerator beam pipes and TFD-SSD are evacuated. Seven o-rings seal the system in order to keep it evacuated. Two o-rings in the plunger, one o-ring beneath the lid, and another above the base prevent gas leaks at the top and bottom of the fixed cylinder. The fifth o-ring lies around the perimeter of the opening through which the beam pipe to the TFD-SSD swings, preventing a leak there. The sixth and seventh o-rings lie on the flanges of the incoming and outgoing beam pipes, sealing the RSC-accelerator and RSC-detector connections. Second, scattering angles between  $0^\circ$  and  $60^\circ$  were desired. Therefore, the fixed cylinder contains an opening which allows the centerline of the beam pipe to the TFD-SSD to swing  $60^\circ$ . The capacity for at least three different scattering foils connected to the plunger was a third requirement. The fixed cylinder is designed to be 9 in tall, and this height accommodates the use of five foils. Finally, friction between the fixed cylinder and collar, both made of aluminum, needed to be minimized to reduce binding and erosion of these parts. To satisfy this requirement, a thin teflon layer

(clamped by aluminum bands) lines the portion of the cylinder around which the collar will rotate. Thus, the collar and cylinder will not make contact during rotation.

The drawings shown in Figs. 10-13 have been submitted to the Physics Machine Shop for construction. The experimenters are awaiting completion of the RSC so that TFD-SSD experiments with the Van de Graaff accelerator can safely ensue.

#### **4. CONCLUSION**

In summary, a 10-layer thin film was fabricated and tested in the TFD-SSD using fission fragments from a Cf-252 source. Signals from both the TFD and SSD were obtained, yielding graphs of counts vs. specific luminescence and counts vs. residual energy, respectively. A rotating scattering chamber was also designed to reduce the intensity of the beam from the Van de Graaff accelerator. The experimenters are awaiting its construction.

Improvements are currently underway to refine the detector's resolution and verify its ionic charge detection. As mentioned earlier, the signal from the thin films currently used are too weak and result in experimental error. To rectify this problem, the experimenters are attempting to create a thin, self-supporting copper thin film that they believe will yield a much stronger signal. Once the RSC is built and implemented, ionic charge detection experiments will be facilitated greatly through enhanced use of the Van de Graaff accelerator. If perfected, the TFD-SSD cosmic ray identifier would make an excellent candidate for instrumentation sent on a space mission to collect cosmic ray data, for which the experimenters ultimately hope to use the detector.

#### **5. ACKNOWLEDGEMENTS**

The author would like to acknowledge Drs. Luis and Barbara Muga and Dr. Dunnam for their guidance, encouragement, and support and Brad Smrstick for his assistance in

designing the RSC. Also, acknowledged are the NSF and University of Florida for financially supporting the REU program and Drs. Ingersent and Dorsey for allowing the author to participate in it.

## 6. REFERENCES

- [1] B. Rossi, *Cosmic Rays* (McGraw-Hill Book Company, New York, 1964).
- [2] V. L. Ginzburg and S. I. Syrovatsky, *Journal of Theoretical Physics (Supplement)* **20**, 1 (1960).
- [3] L. Muga, *Nuclear Instruments and Methods* **124**, 542 (1975).
- [4] Z. Milosevich, M. L. Muga, R. L. Coldwell, and G. J. Bamford, *Nuclear Instruments and Methods in Physics Research* **A320**, 471 (1992).
- [5] G. Friedlander, J. Kennedy, and J. Miller, *Nuclear and Radiochemistry*, 2<sup>nd</sup> ed. (John Wiley and Sons, Inc., New York, 1964), p. 19.